International Journal of Engineering and Geosciences
https://dergipark.org.tr/en/pub/ijeg
e-ISSN 2548-0960

GIS based spatial decision-making approach for solar energy site selection, Ardabil, Iran

Meysam Hasanzadeh [*1], **Khalil Valizadeh Kamran** [1], **Bakhtiar Feizizadeh** [1], **Sanam Hassanzadeh Mollabashi** [2]

[1] *University of Tabriz, Department of Remote Sensing and GIS, Iran, meysam.hasanzadeh@yahoo.com, valizadeh@tabrizu.ac.ir, Feizizadeh@tabrizu.ac.ir*
[2] *University of Shahid Beheshti, Department of Civil and Environment Engineering, Iran, S_hassanzadeh@sbu.ac.ir*

Cite this study: Hasanzadeh, M., Kamran, K. V., Feizizadeh, B., & Mollabashi, S. H. (2024). GIS based spatial decision-making approach for solar energy site selection, Ardabil, Iran. International Journal of Engineering and Geosciences, 9 (1), 115-130

https://doi.org/10.26833/ijeg.1341451

Keywords
AHP
Site Selection Analysis
MCDA
Renewable Energy

Research Article

Received:11.08.2023
Revised: 05.11.2023
Accepted:14.11.2023
Published:02.01.2024

Abstract

Fossil fuel emissions have caused immense harm to the environment, making renewable energy sources like solar power essential. However, finding the optimal location for a solar power plant requires multi-criteria decision analysis (MCDA) due to various factors influencing the selection process. This study used the AHP method to weigh criteria such as GHI, Temperature, Elevation, Slope, Land cover, Distance from city, and Distance from road. The layers created from satellite imagery were combined using algebraic sums to produce a final map with 9 classes The analysis showed that class 9 has the most desirable values for each criterion, indicating the most suitable regions for a solar power plant. The results of the study have identified the southern and some central regions of Ardabil province as being the most suitable location for the construction of a solar power plant. These regions have been found to have favorable values for the criteria studied, indicating a higher potential for solar energy generation. Based on the criteria assigned to class 9, the best lands have been identified, occupying a total area of 3085 hectares. This area represents approximately 0.17% of the total area of Ardabil province. These findings highlight the importance of careful site selection for solar power plants to ensure maximum efficiency and sustainability.

1. Introduction

Environmental pollution and global warming pose a great threat to our planet [1]. The Energy Information Administration (EIA) predicts a 50% increase in global energy consumption between 2018 and 2050 [2], highlighting the need for a shift towards renewable energy sources due to the harmful effects of fossil fuels [3]. Many countries are adopting strategies to transition to low-carbon economies and use clean, environmentally-friendly energy sources [4]. The Paris Agreement, which promotes innovations and solutions for addressing climate change, calls for an increase in renewable energy use [5].

One of the most important sources of renewable energy is solar energy. The main advantages of solar energy systems are reliability, low utilization costs, economic and easy maintenance, free energy source, clean energy, availability, production close to the consumer, low environmental impact, lower emission of greenhouse gases and silence. In contrast, the main disadvantages include high initial cost, large installation area, high dependence on technological development and weather conditions [6].

Solar energy is the third most important source of renewable energy after hydropower and wind power, and its use is increasing [7]. Iran has a high potential for solar energy production [8], and efforts are being made to increase its use to reduce fossil fuel dependence and air pollution. Solar power plants are large-scale installations covered with solar panels that convert solar radiation into electricity [9]. The benefits of solar technology have exponentially increased the installation capacity of solar energy systems between 1992 and 2020 [10]. Geographic information systems (GIS) are commonly used together with multi-criteria decision analysis (MCDA) to determine the optimal locations for constructing solar power plants and performing spatial analysis [3,11-12]. The Analytical Hierarchy Process (AHP) is a commonly used tool in various MCDA methods

to evaluate the suitability of sites for constructing solar power plants.

Various studies have utilized GIS and AHP methods to determine suitable locations for solar power plants [5, 13-17]. Taiar et al. [18] evaluated suitable locations for large-scale solar power plants in Iraq using GIS, hierarchical analysis methods, and TOPSIS. Watson and Hudson [19] used a combination of GIS and AHP to identify the most suitable locations for photovoltaic systems in southern England. Fuzzy logic and AHP have been used in integrated methods to evaluate the suitability of PV systems in Iran [20-21], Türkiye [5], South Korea [22], and Spain [23].

Criteria selection is an important step in any site suitability assessment process for photovoltaic systems. Table 1 shows the criteria considered in some previous studies that have analyzed site suitability for photovoltaic systems.

Table 1. Different criteria considered in previous similar studies on suitability of solar power plant site.

Source	A	B	C	D	E	F	G	H	I
[1]	✓	✓	✓	✓	✓	✓	✓	✓	
[3]	✓		✓	✓	✓	✓	✓	✓	✓
[14]			✓	✓		✓			✓
[19]			✓			✓	✓	✓	✓
[20]			✓	✓	✓		✓	✓	✓
[21]	✓	✓	✓		✓	✓	✓	✓	✓
[22]	✓	✓	✓				✓	✓	✓
[23]	✓	✓	✓			✓	✓	✓	✓

A: Global horizontal irradiance, B: Temperature, C: Slope, D: Aspect, E: Elevation, F: Distance from urban areas, G: Distance from road, H: Distance from power lines, I: Land cover

According to reports published by the International Renewable Energy Agency (IRENA) on March 20th, 2023, the total global installed capacity of renewable energy by 2022 is 3,371,793 MW. Solar power plants are 31% of this capacity with 1,053,115 megawatts. Fourteen Middle Eastern countries have allocated 0.85% of the world's capacity to themselves with a total installed capacity of 28,539 megawatts. Among Middle Eastern countries, Iran has received the first rank with an installed capacity of 12,045 megawatts, followed by Israel with 4,470 megawatts and the United Arab Emirates with 3,058 megawatts. Due to the fact that so far, no published research has investigated the location of solar photovoltaic power plant specifically in Ardabil province, the present research was conducted with the aim of classifying and determining the degree of suitability in each point of the province for placing solar panels. The purpose of determining the best place for the construction of a solar power plant in this province is to increase the annual production of electrical energy, which reduces the investment return time and also reduces investment costs.

In this study, various criteria were considered to assess the suitability of locations for building a solar power plant, and each criterion was prepared as a raster layer. Necessary preprocessing was performed on the layers, and they were normalized. The normalization of the layers was modified compared to conventional methods such as fuzzy membership by using the Python programming language and the Arcpy package. This was done because different normalization methods in ArcMap software have limitations that can produce undesired and, in some cases, incorrect results, based on defined conditions. MCDA was employed to determine the optimal locations. In this research, certain areas of the province within the studied layers were identified as restricted areas according to predetermined conditions and were therefore excluded from the study.

2. Method

Ardabil province is located in the northwest of Iran with an area of 17799 km^2. Due to its longitudinal shape (Figure 1), the province experiences significant climate diversity, with relatively cold and dry conditions in the southern and central regions and relatively warm and semi-moist conditions in the northern parts. According to the Meteorological Organization of Ardabil Province, the province receives more than 2,497 hours of sunshine annually [24].

For the purpose of this research, certain areas were excluded and considered as restricted areas. These included all water bodies such as dams, lakes, and rivers, along with a 200-meter buffer. Additionally, areas with ice and snow, flooded vegetation, forest areas, cities with a buffer of 4 kilometers from Ardabil city and 2 kilometers from other cities, areas with a distance of more than 20 kilometers from them, and all other built-up areas, such as rural and industrial towns, airports, military areas, and all other enclosed areas with a 100-meter buffer were also excluded. These areas were extracted from the land cover map, relevant buffers were applied, and during the classification operation of the land cover layer, they were assigned to the zero class. As a result, they received a zero value in the normalization stage using the linear method.

In this research, seven criteria were considered to determine the optimal location for the construction of a solar power plant in Ardabil, based on the availability of relevant data at the provincial scale. These criteria include global horizontal irradiance (GHI), temperature, elevation, slope, distance from road, distance from city, and land cover.

2.1. The criteria examined

2.1.1. Global Horizontal Irradiance (GHI)

Solar radiation is a critical factor in determining the best location for a solar power plant. It is important to choose locations that receive sufficient sunlight throughout the year [25]. In previous studies, by Martins et al. [26], Amillo et al. [27], and Huld [28], solar radiation was related to global horizontal irradiance, which is also used in this study.

Direct solar radiation is the portion of radiation that reaches a surface directly, while diffuse radiation is the portion that is scattered by the atmosphere. Global radiation is the sum of scattered and direct components that reach a surface. The term solar radiation refers to

the total energy per unit area received from the sun over a specific period of time. Figure 2 presents an overview of the estimated solar energy available for electricity generation and other energy applications. It also displays the long-term average annual/daily total global horizontal irradiance (GHI) [29].

Figure 1. Map of the study area, Ardabil Province.

Based on the report by the National Renewable Energy Laboratory (NREL), areas with solar radiation less than 3.56 kWh/m^2 are not considered economically efficient, and as a result, these areas were not investigated in this research [30]. The GHI value for the Ardabil province ranges from 3.361 kWh/m^2 at the lowest point to 5.012 kWh/m^2 at the highest point. Figure 2 indicates that the northern region of the province has less potential for solar radiation compared to the southern region, and contrary to popular belief, the southern cities of Givi and Khalkhal have significant solar radiation potential.

2.1.2. Temperature

The temperature of photovoltaic cells is a crucial factor in their performance. High-temperature areas can have a negative impact on energy production [31]. The optimal temperature range for solar energy production is below 25°C, and for every 1°C increase in temperature, there is a corresponding decrease in output power of 0.4 to 0.5 percent [32].

The average annual temperature in the Ardabil Province ranges from -9.3°C in the coldest areas to 16.6°C in the hottest regions. The map in Figure 3 indicates that the northern region of the province has a lower potential for temperature compared to the central and southern regions. However, based on the minimum and maximum values associated with the average annual temperature of the province (Figure 3), all parts of the province are suitable in terms of temperature. The value of pixels will increase linearly as the temperature decreases.

2.1.3. Elevation

Higher elevations have the potential to receive more solar radiation compared to lower areas [32]. The elevation of a region above sea level is inversely related to the density of the atmosphere. As the density of the atmosphere increases, the concentration of absorbing or reflecting agents also increases. Since the coarser materials are located in the lower layers, the atmosphere is sparser at the top of mountains. Therefore, high areas have more potential for solar energy production.

However, it should be noted that as the elevation of an area increases, the cost and difficulty of transferring infrastructure and labor also increase [33].

In this research, areas with elevations lower than zero (i.e., below sea level) were removed due to the reduction in solar panel performance. Areas with elevations higher than 2000 meters were also excluded due to the increase in construction costs (Figure 4).

2.1.4. Slope

Increasing the slope of the land can increase the cost of construction and make it more difficult. According to studies conducted by Tahri et al. [33], the maximum acceptable slope for solar power plant construction is 25% or 14 degrees. Therefore, for this research, the maximum allowed slope was set at 15 degrees (Figure 5).

2.1.5. Land cover

In this research, bare ground, pastures, and farms were considered and classified from the most important to the least important land covers, while the rest of the covers, designated as restricted areas, were excluded (Table 2, Figure 6). Built-up areas, flooded vegetation, snow, ice, trees, and water were classified as unsuitable for solar power plant construction, and therefore were assigned a value of zero.

Bare ground was classified as the most suitable because it is economical and readily available. Farms and pastures were classified between these two classes, based on economic and environmental considerations.

2.1.6. Distance from city

Studies conducted by AlGarni and Awasthi [31] and Al-Shammari et al. [34] have removed areas more than 50 km away from built-up areas to determine the optimal location for a solar power plant. However, in this research, areas with a distance more than 20 km away were removed to reduce transportation and construction costs, and to provide cheaper electricity supply to cities (Figure 7).

2.1.7. Distance from road

In the study conducted by Masoom et al. [35], the maximum distance of 50 km from roads was considered to determine the optimal location for a solar power plant, and a distance of 500 m from the center of roads was designated as the road boundary and excluded as restricted areas. Areas far from roads were deemed unsuitable and uneconomical for construction. In this research, areas with a distance greater than 2 km from roads were excluded, and a distance of 100 m from the center of roads was considered as the road boundary and removed (Figure 8). Table 3 provides specifications for all the mentioned criteria.

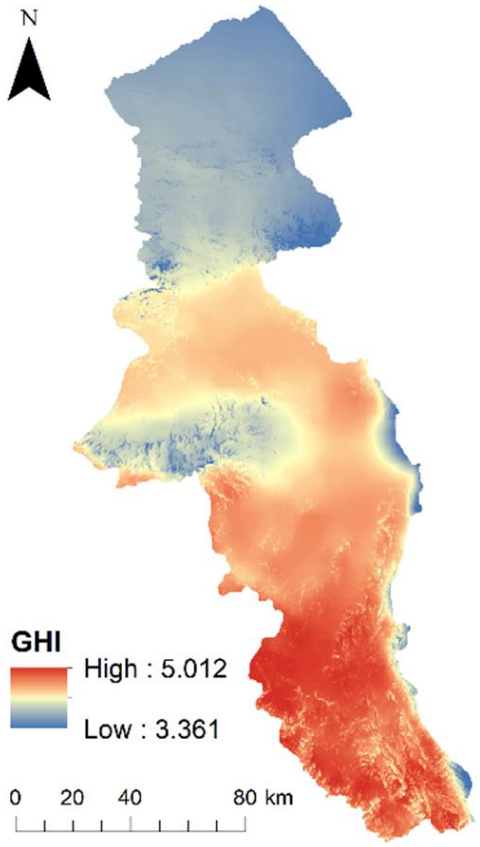

Figure 2. Global horizontal radiation map of Ardabil Province (kwh/m^2).

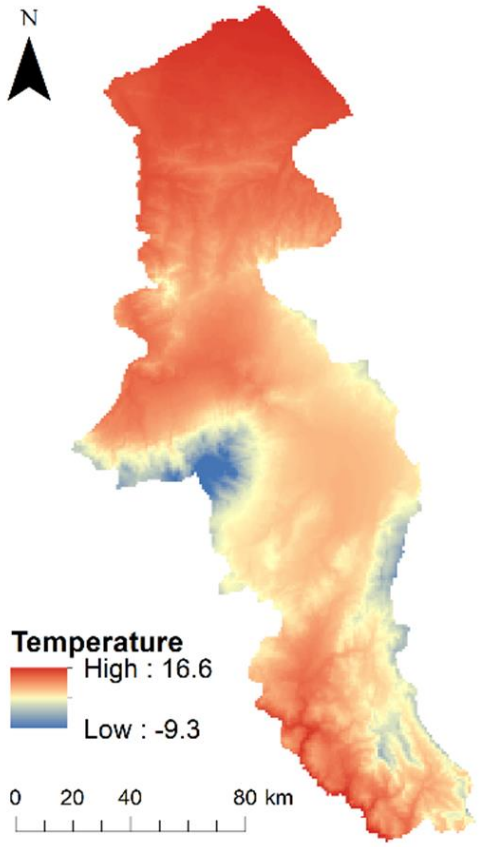

Figure 3. Average annual temperature map of Ardabil Province (°C).

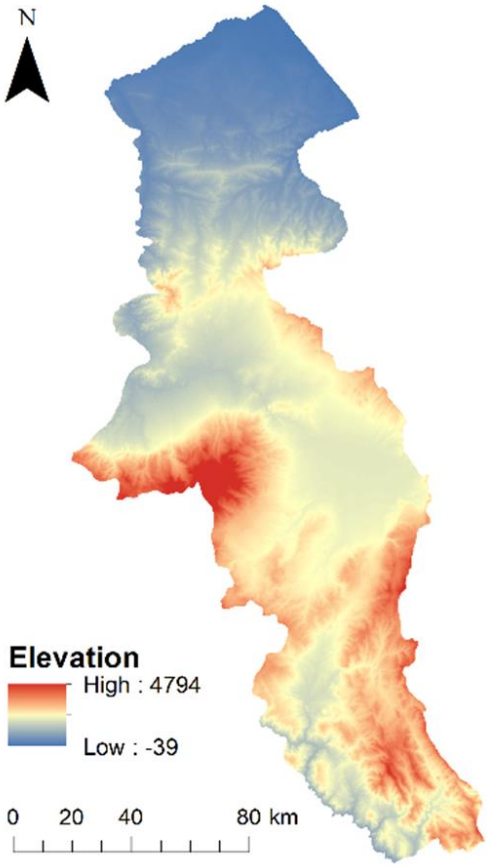

Figure 4. Digital elevation model map of Ardabil Province (m).

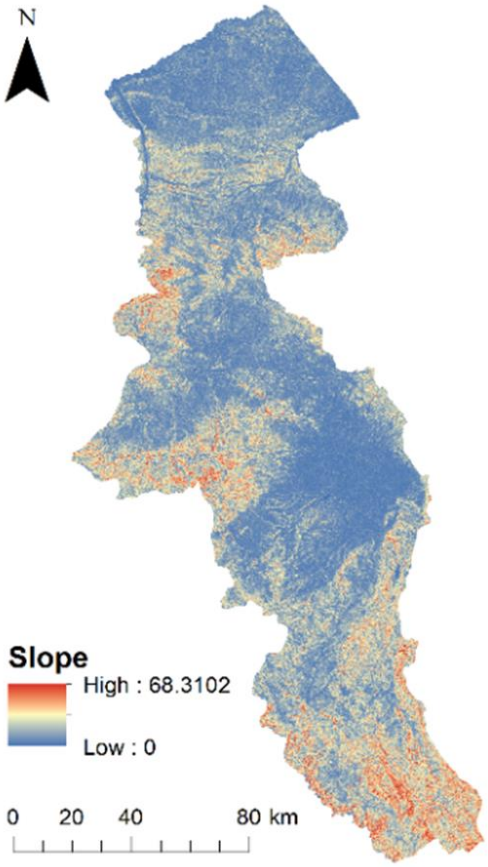

Figure 5. Slope map of Ardabil Province (Degree).

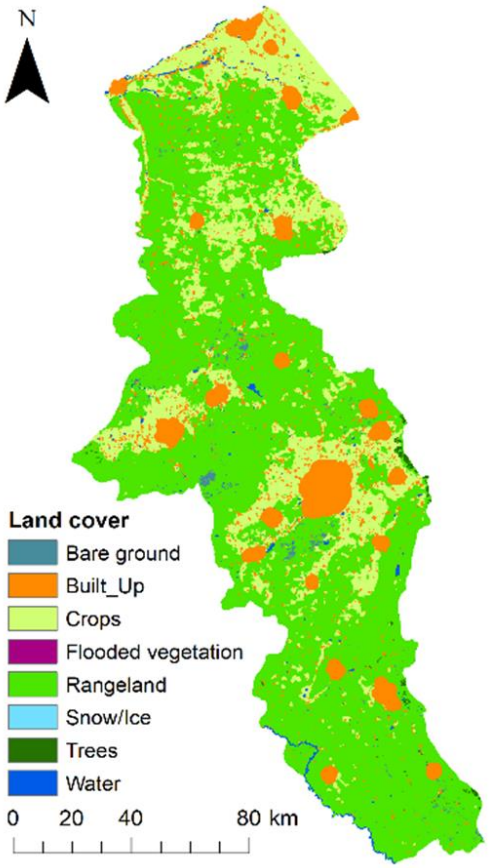

Figure 6. Land cover map of Ardabil Province.

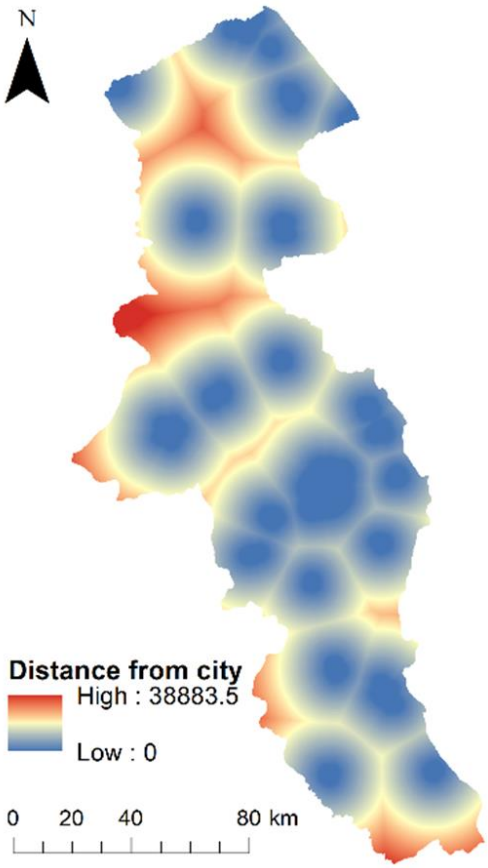

Figure 7. Distance from city map of Ardabil Province (km).

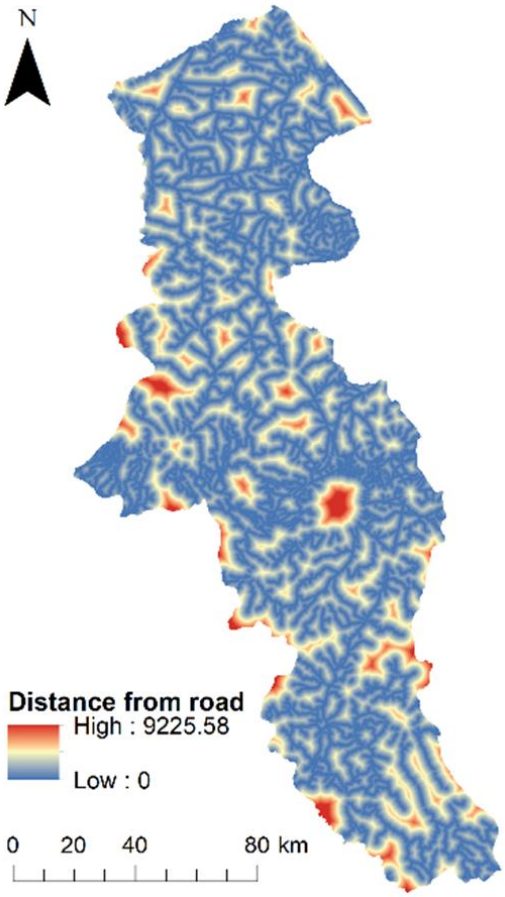

Figure 8. Distance from road map of Ardabil Province (m).

Table 2. Classes related to land cover in Ardabil province.

0	1	2	3
Built-up areas Flooded vegetations Snow and ice Trees Water	Farms	Pastures	Bare ground

This research uses MCDA method. the layers were normalized using a modified linear fuzzy logic, coded using the Arcpy package in ArcMap. This involved assigning a value of one to pixels with the maximum degree of desirability and a value of zero to unsuitable pixels, with the remaining pixels assigned values between these two extremes. The weight of each parameter was determined using the AHP weighting technique, and the normalized layer was multiplied by its respective weight. Pixels with a value of zero were removed, and the final layer was produced by summing the values of the pixels in each investigated layer. The final layer was classified into 9 classes to preserve valuable information and maintain accuracy, while avoiding the creation of empty or useless classes.

To validate the model, two points were selected from classes 9 and 3, and the corresponding values of each layer were extracted. ArcMap 10.2 software (ESRI) was used for data processing and analysis. Maps related to distance from city and road were converted from vector format to raster using the Euclidean distance tool. The spatial resolution of the layers was resampled to 28.40590591 to match the spatial resolution of the Digital Elevation Model (DEM) image, while considering the extent of the studied area.

Table 3. Specifications of the investigated parameters.

	Data	Spatial Resolution	Reference	Format
Climate	GHI	250 m	Global Solar Atlas- Solar GIS [29]	Raster
	Temperature	800 m	Global Solar Atlas- Solar GIS [29]	Raster
Geomorphological	Elevation	28.406 m	Nasa Earth Data [36]	Raster
	Slope	28.406 m	Nasa Earth Data [36]	Raster
Spatial	Distance from city	28.406 m	Esri Global Land Use [37]	Vector
	Distance from road	28.406 m	OSM [38]	Vector
Environmental	Land cover	10 m	Esri Global Land Use [37]	Raster

2.2. Data standardization

Considering that each parameter can have a unique range, normalization should be conducted in order to use them in multi criteria evaluations. Fuzzy normalization standardizes input layers on a scale of 0 to 1 [22]. To evaluate the degree of membership of a parameter in a fuzzy set, several types of fuzzy functions have been developed and published in scientific literature (Equation 1) [39].

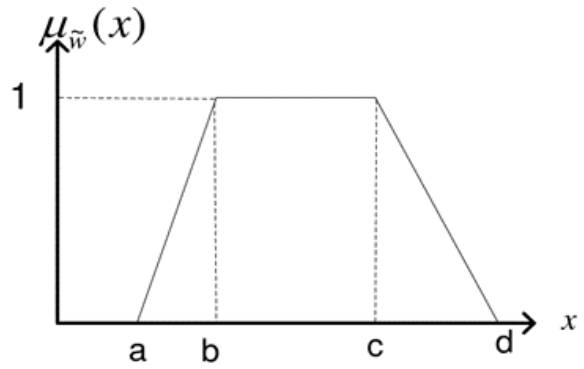

Figure 9. Linear fuzzy logic function (x, parameter; u(x), degree of fuzzy membership) [40].

$$\text{trapezoid}(x; a, b, c, d) = \begin{cases} 0, & x \le a. \\ \dfrac{x-a}{b-a}, & a \le x \le b. \\ 1, & b \le x \le c. \\ \dfrac{d-x}{d-c}, & c \le x \le d. \\ 0, & d \le x. \end{cases} \quad (1)$$

Due to the limitations in the linear fuzzy logic set of ArcMap, it was decided to code this linear function in Python programing language in this software using Arcpy package. For example, while normalizing the elevation layer of the province, by increasing elevation to 2000m, the value of the pixels increased, where pixels with elevation of 2000 got the value one. Elevations more than 2000 have been excluded from this research, but using the linear fuzzy logic membership set ready in ArcMap software, the areas with elevation more than 2000 are also assigned a value of one, and this issue is contrary to the intended criterion in this study. According to this issue, the normalization of the layers in the GIS environment was coded using the linear fuzzy logic method.

The normalization of the GHI layer of the province is done in order that the pixels that have radiation between 3.56 kwh/m^2 and 5.012 kwh/m^2 are assigned values between zero and one, so that with the increase in the amount of radiation, the value of pixels increase and get one. Considering that the maximum amount of global horizontal radiation in the province is 5.012 kwh/m^2, the pixels with this value are assigned the value of one after applying the normalization functions. Pixels with radiation of 3.56 kwh/m^2 and less receive zero value.

Also, in the normalization of the temperature layer of the province, the pixels with the temperature between -9.3 and 16.6 °C are assigned values between zero and one, so that with the decrease in temperature, the value of the pixels increases and reaches a value of one. pixels with temperature -9.3°C is assigned a value of one and a pixel with a temperature of 16.6 is assigned a value of zero.

Pixels with an elevation between 0 and 2000 m above sea level are assigned values between 0 and 1. As the elevation increases, the value of the pixels increases and approaches the value of one, so that pixels with a height of zero and less have a value of zero and pixels with a height of 2000 m are assigned a value of 1. Those with an elevation of more than 2000 m are excluded from this study due to their high elevation and increased construction costs, and are assigned a value of zero.

Pixels with a slope between 0 and 15 degrees received values between zero and one, and as the slope decreases, the value of pixels increases and approaches the value of one. Pixels with a slope of 15 degrees and more have a value of zero, and pixels with a slope of zero degrees have a value of one.

Class 3 land cover layer, which corresponds to rocky or soil areas with very little or no vegetation cover during the year, such as rock or soil, desert and dunes, salt marshes, dry hills and dried lakes, has the highest value in this research and they are assigned a value of one, while the uses of built-up areas, water areas, forest areas, and areas with ice and snow, which are assigned to the zero class, will be taken as zero after normalization and will be removed.

As the distance from cities increases, the value of pixels decreases. Pixels that have a distance of 20 km or more from the considered city (which its boundary is determined using the special mentioned buffer) have a value of zero, and as the distance from city limits decreases, its value gets closer to one.

As the distance from road increases, the value of the pixels decreases. Pixels that have a distance of 2 km or more from the center of the road have a value of zero, and the closer we get to a distance of 100m from the center of the road, the value becomes closer to one. Pixels with distance equal to and less than 100m from the center of the road receive value of zero.

2.3. Using AHP technique in layer weighting

AHP technique was first proposed by Saaty [41] and consists of a system that compares a number of variables by determining the weight of importance of a factor relative to each factor considered. Pairwise comparison refers to the process of comparing several factors or elements in pairs to decide which factor is preferable (relative importance) or whether two factors are equally important in a particular problem. Thus, it simplifies a complex problem and facilitates the determination of reasonable weights for multiple factors. In a pairwise comparison, the sum of the weights of all criteria is 1. For example, in the case of four criteria (i.e., factors A-D), a 4x4 matrix is needed to determine the weights of the four criteria (Equation 2).

Each element of the pairwise comparison matrix represents the relative importance value of one factor to another, assigned using the 1-9 scale of importance intensity described in Table 4. For example, if factor A is more important than factor B in predicting a subsidence event, CAB is assigned a relative intensity value of 5. Since the matrix is symmetric, only the upper triangular half of the pairwise comparison matrix needs to be completed. The remaining elements are reversed of upper half-triangular. The value of the diagonal elements of the matrix is one.

Once all the values of the pairwise comparison matrix elements were determined, a normalized matrix with respect to the number of criteria can be calculated based on Equation 3:

where each element represents the weighted value of each criterion. The relative weight for each factor is determined in the range of 0 to 1. A higher weight indicates a greater contribution of this factor to PV suitability.

$$\text{Matrix: } \begin{bmatrix} C_{11} & C_{12} & C_{13} & C_{14} \\ C_{21} & C_{22} & C_{23} & C_{24} \\ C_{31} & C_{32} & C_{33} & C_{34} \\ C_{41} & C_{42} & C_{43} & C_{44} \end{bmatrix} = \begin{bmatrix} 1 & C_{AB} & C_{AC} & C_{AD} \\ C_{BA} & 1 & C_{BC} & C_{BD} \\ C_{CA} & C_{CB} & 1 & C_{CD} \\ C_{DA} & C_{DB} & C_{DC} & 1 \end{bmatrix} \quad (2)$$

$$P = \begin{bmatrix} p_1 \\ p_2 \\ p_3 \\ p_4 \end{bmatrix} = \begin{bmatrix} \omega_A \\ \omega_B \\ \omega_C \\ \omega_D \end{bmatrix} = \frac{1}{4} \times \begin{vmatrix} \sum_{j=1}^{4} \frac{C_{1j}}{C_{0j}} \\ \sum_{j=1}^{4} \frac{C_{2j}}{C_{0j}} \\ \sum_{j=1}^{4} \frac{C_{3j}}{C_{0j}} \\ \sum_{j=1}^{4} \frac{C_{4j}}{C_{0j}} \end{vmatrix} \quad \text{where } C_{0j} = \sum_{i=1}^{4} C_{ij} \quad (3)$$

Table 4. Degree of importance in pairwise comparisons.

Importance	Definition	Explanation
1	Equal importance	The two activities contribute equally to the goal
3	Medium importance	A little experience and judgment prefer one activity over another
5	Strong importance	Experience and judgment strongly prefer one activity over another
7	Very strong or demonstrated importance	One activity is strongly preferred over another. Its domination was demonstrated in practice
9	Too much importance	Evidence that prefers one activity over another has the highest possible degree of confirmation
2,4,6,8	Intermediate values	
The reverse of the above		In the case of inverse comparison of the relationship between elements, the reversed values are assigned a degree of importance

To identify the degree of consistency in the assignment of element values in the pairwise comparison matrix, the consistency ratio (CR) can be used. CR shows the consistency of the participants opinions in scoring the pairwise comparison matrix. CR is defined as the ratio between the consistency index (CI) (Equation 5) of the matrix and a randomness index (RI) shown in Equation 6. As reported by Ishizaka and Labib [42], RI can be assigned based on the number of criteria, using an appropriate value. In general, a CR value of less than 0.1 is considered to indicate a valid comparison.

$$M = C \times P = \begin{bmatrix} m_1 \\ m_2 \\ m_3 \\ m_4 \end{bmatrix} \quad (4)$$

$$CI = \frac{\left(\frac{\sum_{i=1}^{4} \frac{m_i}{p_i}}{4} \right) - 4}{4 - 1} \quad (5)$$

$$CR = CI/RI \quad (6)$$

When expert's judgments differed for a particular element of the comparison matrix, geometric mean values were used to combine the preferences for each element to minimize the multiplicative error in computing the comparison matrix, as suggested by Ishizaka and Labib [42].

2.4. Determining the weights of the criteria using the AHP method

According to the previous studies and researches in the field of solar power plant location [3-4,22], considering the social and economic conditions of Iran and Ardabil province and judgments between criteria gathered from a group of experts related in solar energy, the degree of importance of the criteria was determined in Table 5. By dividing the elements of each column by the sum of the columns, the normal matrix of pairwise comparisons is made according to Table 6. By averaging each row of the normal matrix of pairwise comparisons, the weight of each criterion is acquired, shown in Table 7.

In order to calculate the consistency rate, we first multiply each element of the primary matrix column (Table 5) by the weight of each criterion (Table 7). The sum of each row of the acquired matrix is called the weighted sum of values. Finally, we divide the obtained weighted sum of values by the weight of each criterion, which we name the corresponding as column A (Table 8).

Table 5. Matrix of pairwise comparisons.

AHP	GHI	Slope	Distance from road	Distance from city	Elevation	Land cover	Temperature
GHI	1	2	3	4	5	6	7
Slope	1/2	1	2	3	4	5	6
Distance from road	1/3	1/2	1	2	3	4	5
Distance from city	1/4	1/3	1/2	1	2	3	4
Elevation	1/5	1/4	1/3	1/2	1	2	3
Land cover	1/6	1/5	1/4	1/3	1/2	1	2
Temperature	1/7	1/6	1/5	1/4	1/3	1/2	1

Table 6. Normal matrix of pairwise comparisons.

AHP	GHI	Slope	Distance from road	Distance from city	Elevation	Land cover	Temperature
GHI	0.3857	0.4494	0.4119	0.3609	0.3158	0.2791	0.2500
Slope	0.1928	0.2247	0.2746	0.2707	0.2526	0.2326	0.2143
Distance from road	0.1286	0.1124	0.1373	0.1805	0.1895	0.1860	0.1786
Distance from city	0.0964	0.0749	0.0686	0.0902	0.1263	0.1395	0.1429
Elevation	0.0771	0.0562	0.0458	0.0451	0.0632	0.0930	0.1071
Land cover	0.0643	0.0449	0.0343	0.0301	0.0316	0.0456	0.0714
Temperature	0.0551	0.0375	0.0275	0.0226	0.0211	0.0233	0.0357

Table 7. The weight of each criterion.

GHI	Slope	Distance from road	Distance from city	Elevation	Land cover	Temperature
0.3504	0.2375	0.1590	0.1056	0.0696	0.0462	0.0318

Table 8. Weighted sum of values.

AHP	GHI	Slope	Distance from road	Distance from city	Elevation	Land cover	Temperature	Weighted total values	A
GHI	0.3504	0.4750	0.4770	0.4224	0.3480	0.2772	0.2226	2.5726	7.341894977
Slope	0.1752	0.2375	0.3180	0.3168	0.2784	0.2310	0.1908	1.7477	7.358736842
Distance from road	0.1168	0.1188	0.1590	0.2112	0.2088	0.1848	0.1590	1.1584	7.285220126
Distance from city	0.0876	0.0792	0.0795	0.1056	0.1392	0.1386	0.1272	0.7569	7.16729798
Elevation	0.0701	0.0594	0.0530	0.0528	0.0696	0.0924	0.0954	0.4927	7.078376437
Land cover	0.0584	0.0475	0.0398	0.0352	0.0348	0.0462	0.0636	0.3255	7.044372294
Temperature	0.0501	0.0396	0.0318	0.0264	0.0232	0.0231	0.0318	0.2259	7.105046421

By averaging the values of column, A, λ is acquired:

$\lambda = 7.1972$

Then it's time to calculate the C.I consistency index:

$C.I=(\lambda-8)/7$
$C.I=0.0328$

The consistency rate or C.R is obtained by dividing the consistency index C.I by R.I, which R.I is determined according to the number of criteria and Table 9:

$C.R = C.I / R.I$
$C.R = 0.0249$

Considering that the consistency rate is 0.0249 and is less than 0.1, it can be concluded that the acquired weight values are acceptable and the criteria are logically compatible.

Table 9. The value of R.I based on the number of criteria.

n	1	2	3	4	5	6	7	8	9	10
R.I	0	0	0.58	0.9	1.12	1.24	1.32	1.41	1.45	1.49

In order to normalize the layers, Python programming language was used in the GIS environment. The package used is Arcpy and the module used is Arcpy.sa (Spatial Analyst), which is a module for raster and vector data analysis with the capacity provided by the ArcGIS Spatial Analyst extension. This module provides access to all the geoprocessing tools in the Spatial Analyst toolbox, as well as other functions and classes that allow you to automate your raster processing workflows [44]. Codes used for the linear normalization of the layers are presented in Table 10. It should be noted that if, for example, a pixel has all the appropriate conditions and is inappropriate only in terms of one criterion, meaning its value is zero after normalization, then that pixel is considered inappropriate and is not classified in any of the classes of the final layer. For this purpose, before overlaying the layers, the pixels that received zero value after normalization and weighting will be removed using the Raster Calculator tool and the Set Null command. Table 11 includes the commands used to remove pixels with zero values.

Table 10. The normalization scripts of each layer along with the applied weights.

Elevation	>>> import arcpy
	>>> from arcpy.sa import*
	>>> x = Raster ("Elevation")
	>>> ElevationNormalizedMap=Con((x>=0) &(x<=2000), ((x-0)/2000.0),0)
	>>> ElevationWeightedNormalizedMap = ElevationNormalizedMap *0.0696

Slope	>>> import arcpy
	>>> from arcpy.sa import*
	>>> x=Raster("Slope")
	>>> SlopeNormalizedMap =Con((x>=0) &(x<=15), ((15-x)/15.0),0)
	>>> SlopeWeightedNormalizedMap = SlopeNormalizedMap *0.2375

GHI	>>> import arcpy
	>>> from arcpy.sa import*
	>>> x = Raster ("GHI")
	>>> GHINormalizedMap =Con((x>=3.560) &(x<=5.012), ((x-3.560)/1.452),0)
	>>> GHIWeightedNormalizedMap = GHINormalizedMap *0.3504

Temperature	>>> import arcpy
	>>> from arcpy.sa import*
	>>> x = Raster ("'Temperature")
	>>> TemperatureNormalizedMap =Con((x>=-9.3) &(x<=16.6), ((16.6-x)/25.9),0)
	>>> TemperatureWeightedNormalizedMap = TemperatureNormalizedMap *0.0318

Distance From Road	>>> import arcpy
	>>> from arcpy.sa import*
	>>> x = Raster ("DistancefromRoad")
	>>> DistancefromRoadNormalizedMap =Con((x>100) &(x<=2000.0), (2000.0-x)/1900.0, Con((x<=100) &(x>2000),0,0))
	>>> DistancefromRoadWeightedNormalizedMap = DistancefromRoadNormalizedMap *0.1590

Distance From City	>>> import arcpy
	>>> from arcpy.sa import*
	>>> x = Raster ("DistancefromCity")
	>>> DistancefromCityNormalizedMap =Con((x>0) &(x<=20000.0), (20000.0-x)/20000.0, Con((x<=0) &(x>20000),0,0))
	>>> DistancefromCityWeightedNormalizedMap = DistancefromCityNormalizedMap *0.1056

Landcover	>>> import arcpy
	>>> from arcpy.sa import*
	>>> x = Raster ("Landcover")
	>>> LandcoverNormalizedMap =Con((x>=0) &(x<=3), (x)/3.0,0)
	>>> LandcoverWightedNormalizedMap = LandcoverNormalizedMap *0.0462

Table 11. Command to remove pixels with zero values in each layer after applying normalization functions.

Elevation	SetNull (" ElevationWeightedNormalizedMap " == 0," ElevationWeightedNormalizedMap ")
Slope	SetNull (" SlopeWeightedNormalizedMap " == 0," SlopeWeightedNormalizedMap ")
GHI	SetNull (" GHIWeightedNormalizedMap " == 0," GHIWeightedNormalizedMap ")
Temperature	SetNull (" TemperatureWeightedNormalizedMap " == 0," TemperatureWeightedNormalizedMap ")
Distance From Road	SetNull (" DistancefromRoadWeightedNormalizedMap " == 0," DistancefromRoadWeightedNormalizedMap ")
Distance From City	SetNull (" DistancefromCityWeightedNormalizedMap " == 0," DistancefromCityWeightedNormalizedMap ")
Landcover	SetNull (" LandcoverWightedNormalizedMap " == 0," LandcoverWightedNormalizedMap ")

2.5. Produce the final map

By using the method of summing the pixel values of the layers related to the investigated criteria that are normalized and multiplied by the weight obtained using the AHP technique, the final layer indicating the degree of suitability of each pixel for the construction of a solar power plant is acquired (Equation 7).

$$\text{Suitability index} = \sum(\text{Fuzzy membership index}_i \times \text{Weight}_i) \quad (7)$$

3. Results

Many studies have been conducted to identify suitable sites for solar power plants [45]. The importance of criteria considered in such studies may vary depending on the region's location, environment, climate, geomorphological, economic, and infrastructure conditions, depending on the opinions of specialists and experts. By using multi-criteria decision-making methods, prioritizing criteria using the AHP method, and stacking layers in different ways in the GIS environment, regional location costs for solar power plants can be effectively reduced [1,3-4,22,43, 46]. To increase the use of solar energy, it is essential to achieve cost-effectiveness and reduce the investment return time for investors. Therefore, determining the optimal location for a solar power plant is crucial.

This research uses the algebraic sum method to overlay normalized layers and account for the relative importance of different criteria in determining the suitability of various locations within Ardabil province for the construction of a solar power plant. By normalizing the layers and considering the importance of criteria relative to each other, the research aims to accurately determine the optimal location for a solar power plant in the region. The final map, with pixels divided into nine equal interval classes, is shown in Figure 9. Class 9 refers to the strongest pixels and class 1 refers to the weakest pixels.

The area of each class along with the percentage of its area compared to the total area of the province is shown in the Table 12. This table shows that 59.88% of the area of the province is completely unsuitable for the construction of a solar power plant.

Pixels that are assigned class 9 should be prioritized when planning to build a solar power plant.

As shown in Figure 9, the most suitable areas are located in the south and somehow in the center of the province, which are indicated by classes 9 and 8. This is due to relatively lower temperature and more solar radiation as well as higher altitude. The areas of classes 8 and 9 cover a total area of 78260.3 hectares, equivalent to 4.39% of the total area of the province. Also, the northern regions of the province are mainly allocated to lower classes due to high temperature, lower elevation and lower global horizontal irradiance, which are all three negative factors affecting the location for the construction of a solar power plant.

Table 12. The pixels area of suitability map for Ardabil province, separated by each class, along with the percentage of the area of each class compared to the total area of the province.

Class	9	8	7	6	5	4	3	2	1
Area (Hectares)	3085.81	75174.49	177814.75	183189.32	164937.99	90193.24	19495.24	769.29	1.53
Percentage	0.17	4.22	9.98	10.29	9.26	5.06	1.09	0.0432	0.00008

The solar site suitability analysis performed in this research can be a preventive step to support decision makers in finding and selecting the most suitable locations for the development of PV systems in Ardabil province whether small-scale PV systems or large-scale ones. Large-scale PV systems can be built on certain vacant lands that achieve a high degree of suitability, such as areas assigned to Class 9 as shown in Figure 10.

Table 13 shows the pixel values of each criterion for two points located in classes 9 and 3. Class 9 which represents the best pixels for construction of solar power plant, and land related to this class has higher global horizontal irradiance and elevation, lower slope and temperature and generally shorter distance from road and city. X and Y refer to the coordinates of the desired pixel in UTM (Universal Transverse Mercator) coordinate system, located in zone 39S.

In order to calculate the efficiency of the solar power plant for two points in Table 13, the open-source Global Solar Atlas Energy was used. The type of power plant was selected from the ground mounted large-scale type and the nominal capacity of the power plant was arbitrarily determined to be 10 MW. Results show that land related to class 9 has higher efficiency than land related to class 3, about 24% (Table 10).

The pixel data in Table 13 and Table 14 shows the importance of using AHP weighting method. Considering that according to the opinion of experts in this field, the amount of solar radiation and the slope of the earth are more important, as a result, they have been given more weight. Figure 11 shows the value of each criterion considering two determent points. These charts obviously present the difference between class 9 and 3 of this study.

As a result of processing the received satellite imageries of Ardabil province, related to the seven criteria examined in the GIS environment and their overlaying, the final map produced was classified into 9 classes. It can be concluded that the best land for the construction of a solar power plant according to criteria and conditions, is located mainly in the south and to some extent in the central areas of the province. The best lands

assigned to class 9 occupy 3085 hectares, which is about 0.17% of the area of the province. In general, suggest to use lands assigned to class 9 and then class 8, when deciding to construct a solar power plant considering sustainable development and economic efficiency for investors. The requirement of any sustainable development is the correct choice of location, using site selection techniques and multi-criteria decision-making methods.

Table 13. Pixel values related to random points determined in the examined raster criteria.

Class	9	3
X	268350	262980
Y	4167506	4321501
Temperature (°C)	10.4	11.8
Slope (degree)	3.35	14.18
Distance from Road (m)	204	779
GHI (kwh/m^2)	4.95	4.03
Elevation (m)	1682	821
Distance from City (m)	4484	95
Land cover	Rangeland	Rangeland

Table 14. Calculated Energy yield for two random points.

Class	9	3
X	268350	262980
Y	4167506	4321501
Energy yield of a 10MW installed capacity power plant (GW per year)	16.777	13.562

After investigating the existing solar power plants in Ardabil province, results were obtained that with two solar power plants, each with a capacity of 1 megawatt, it has allocated 0.01% of the total installed capacity of renewable energy to itself in Iran. The power plant located in the south of the province is in classes 8 and 9, while the power plant located in the north of the province is in classes 7 and 8, according to this study.

4. Conclusion

This study used MCDA method to determine the optimal locations to Construct Solar Power plant in Ardabil Province, Iran. Seven criteria considered to be evaluated in this study: GHI, Temperature, Elevation, Slope, Land cover, Distance from city and Distance from road. AHP was used to weight the criteria and then the linear normalization of the layers was done using python programing in ArcMap software. All the pixels that received zero value after normalization were excluded from this study. The final layer was obtained as an algebraic sum of the weighted criteria. The final map produced was classified into 9 classes and indicates that the best lands that belong to class 9 and 8 which are respectively 0.17 and 4.22 percent of the province area, are located in the south and central regions of the province which show the best lands to build a solar power plant and requires multi-criteria decision making.

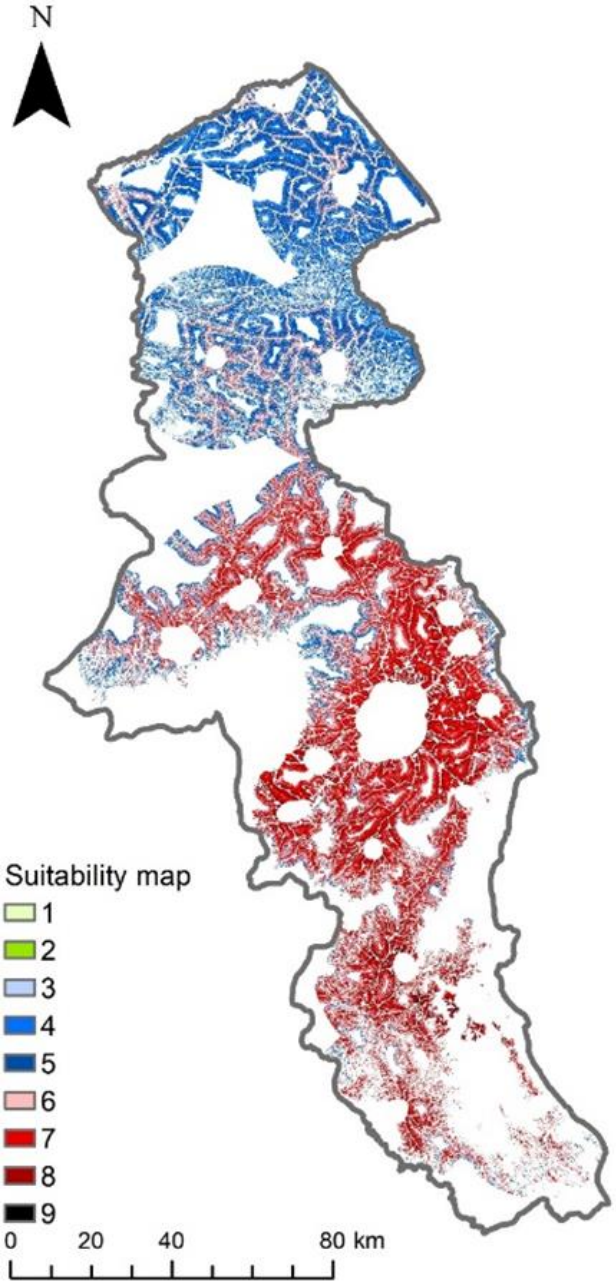

Figure 9. Classified map for the suitability degree of Ardabil province in order to construction of a solar power plant.

Author contributions

Meysam Hasanzadeh: Conducted this research, analyzed results and wrote the manuscript **Khalil Valizadeh Kamran:** Analyzed results **Bakhtiar Feizizadeh:** Edited Scientific and literary **Sanam Hassanzadeh Mollabashi:** Edited Scientific and literary

Conflicts of interest

The authors declare no conflicts of interest.

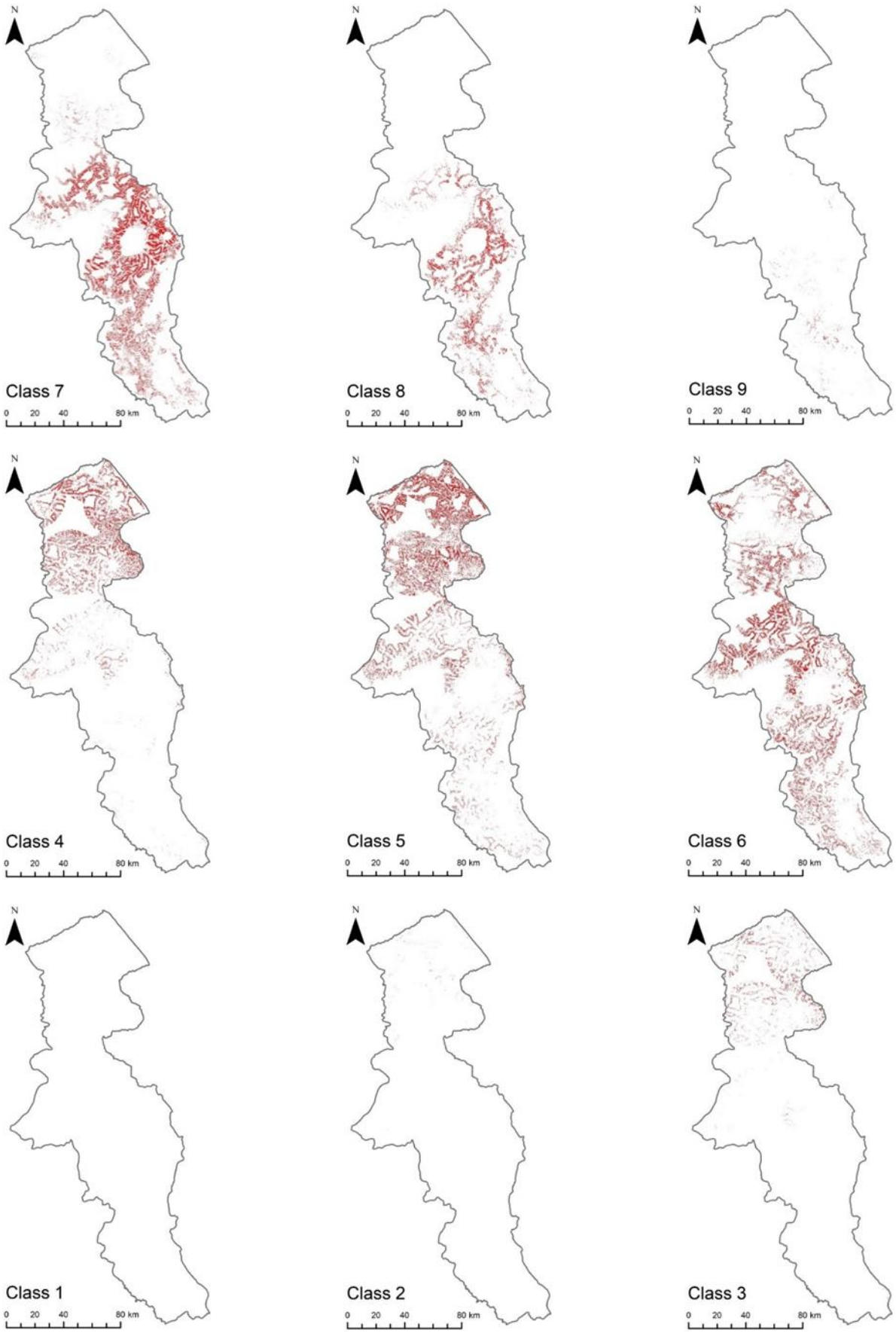

Figure 10. Suitability map of Ardabil province by each class.

Figure 11. Values of each criterion for two random points.

References

1. Albraheem, L., & Alabdulkarim, L. (2021). Geospatial analysis of solar energy in riyadh using a GIS-AHP-based technique. ISPRS International Journal of Geo-Information, 10(5), 291. https://doi.org/10.3390/ijgi10050291
2. U. S. (2021). Energy Information Administration. https://www.eia.gov/todayinenergy/detail.php?id=41433/
3. Gašparović, I., & Gašparović, M. (2019). Determining optimal solar power plant locations based on remote sensing and GIS methods: A case study from Croatia. Remote Sensing, 11(12), 1481. https://doi.org/10.3390/rs11121481
4. Munkhbat, U., & Choi, Y. (2021). GIS-based site suitability analysis for solar power systems in Mongolia. Applied Sciences, 11(9), 3748. https://doi.org/10.3390/app11093748
5. Uyan, M. (2013). GIS-based solar farms site selection using analytic hierarchy process (AHP) in Karapinar region, Konya/Turkey. Renewable and Sustainable Energy Reviews, 28, 11-17. https://doi.org/10.1016/j.rser.2013.07.042
6. Sampaio, P. G. V., & González, M. O. A. (2017). Photovoltaic solar energy: Conceptual framework. Renewable and Sustainable Energy Reviews, 74, 590-601. https://doi.org/10.1016/j.rser.2017.02.081
7. World Energy Outlook (2019). https://www.iea.org/reports/world-energy-outlook-2019.
8. Weather Data and Software for Solar Power Investments. Available online: http://solargis.info/doc/_pics/freemaps/1000px/ghi/SolarGIS-Solar-map-Iran-en.png
9. Shaikh, M. R. S., Waghmare, S. B., Labade, S. S., Fuke, P. V., Tekale, A. (2017). A review paper on electricity generation from solar energy. International Journal for Research in Applied Science & Technology 5(9), 1884-1889. http://dx.doi.org/10.22214/ijraset.2017.9272
10. Rabaia, M. K. H., Abdelkareem, M. A., Sayed, E. T., Elsaid, K., Chae, K. J., Wilberforce, T., & Olabi, A. G.

(2021). Environmental impacts of solar energy systems: A review. Science of The Total Environment, 754, 141989. https://doi.org/10.1016/j.scitotenv.2020.141989
11. Choi, Y., Suh, J., & Kim, S. M. (2019). GIS-based solar radiation mapping, site evaluation, and potential assessment: A review. Applied Sciences, 9(9), 1960. https://doi.org/10.3390/app9091960
12. Genç, M. S., Karipoğlu, F., Koca, K., & Azgın, Ş. T. (2021). Suitable site selection for offshore wind farms in Turkey's seas: GIS-MCDM based approach. Earth Science Informatics, 14(3), 1213-1225. https://doi.org/10.1007/s12145-021-00632-3
13. Doorga, J. R., Rughooputh, S. D., & Boojhawon, R. (2019). Multi-criteria GIS-based modelling technique for identifying potential solar farm sites: A case study in Mauritius. Renewable energy, 133, 1201-1219. https://doi.org/10.1016/j.renene.2018.08.105
14. Ziuku, S., Seyitini, L., Mapurisa, B., Chikodzi, D., & van Kuijk, K. (2014). Potential of concentrated solar power (CSP) in Zimbabwe. Energy for Sustainable Development, 23, 220-227. https://doi.org/10.1016/j.esd.2014.07.006
15. Neisani Samani, N., & Tahouni, A. (2019). The Evaluation of suitable Sites for Solar Farms by Multi Criteria Decision Making in GIS (Case Study: East Azarbaijan Province). Human Geography Research, 51(3), 747-764. https://doi.org/10.22059/jhgr.2019.279885.1007909
16. Piirisaar, I. (2019). A multi criteria GIS analysis for siting of utility-scale photovoltaic solar plants in county Kilkenny, Ireland. [Master's thesis, Lund University].
17. Ruiz, H. S., Sunarso, A., Ibrahim-Bathis, K., Murti, S. A., & Budiarto, I. (2020). GIS-AHP Multi Criteria Decision Analysis for the optimal location of solar energy plants at Indonesia. Energy Reports, 6, 3249-3263. https://doi.org/10.1016/j.egyr.2020.11.198
18. Taiar, A., M. Rezvan, & H. Hashemi. (2019). Evaluation of suitable locations for large-scale solar power plants using GIS, Hierarchical Analysis Process (AHP) and TOPSIS (Case Study: Karbala Province, Iraq). Energy Engineering and Management, 4, 60-73. https://doi.org/10.22052/11.4.60
19. Watson, J. J., & Hudson, M. D. (2015). Regional Scale wind farm and solar farm suitability assessment using GIS-assisted multi-criteria evaluation. Landscape and Urban Planning, 138, 20-31. https://doi.org/10.1016/j.landurbplan.2015.02.001
20. Asakereh, A., Omid, M., Alimardani, R., & Sarmadian, F. (2014). Developing a GIS-based fuzzy AHP model for selecting solar energy sites in Shodirwan region in Iran. International Journal of Advanced Science and Technology, 68, 37-48. http://dx.doi.org/10.14257/ijast.2014.68.04
21. Noorollahi, E., Fadai, D., Akbarpour Shirazi, M., & Ghodsipour, S. H. (2016). Land suitability analysis for solar farms exploitation using GIS and fuzzy analytic hierarchy process (FAHP)—a case study of Iran. Energies, 9(8), 643. https://doi.org/10.3390/en9080643
22. Suh, J., & Brownson, J. R. (2016). Solar farm suitability using geographic information system fuzzy sets and analytic hierarchy processes: Case study of Ulleung Island, Korea. Energies, 9(8), 648. https://doi.org/10.3390/en9080648
23. Sánchez-Lozano, J. M., Teruel-Solano, J., Soto-Elvira, P. L., & García-Cascales, M. S. (2013). Geographical Information Systems (GIS) and Multi-Criteria Decision Making (MCDM) methods for the evaluation of solar farms locations: Case study in south-eastern Spain. Renewable and sustainable energy reviews, 24, 544-556. https://doi.org/10.1016/j.rser.2013.03.019
24. https://ardmet.ir
25. Abdelrazek, M. (2017). GIS Approach to Find Suitable Locations for Installing Renewable Energy Production Units in Sinai Peninsula, Egypt. [Master's thesis, University of Salzburg].
26. Martins, F. R., Pereira, E. B., & Abreu, S. L. (2007). Satellite-derived solar resource maps for Brazil under SWERA project. Solar Energy, 81(4), 517-528. https://doi.org/10.1016/j.solener.2006.07.009
27. Amillo, A. G., Huld, T., & Müller, R. (2014). A new database of global and direct solar radiation using the eastern meteosat satellite, models and validation. Remote sensing, 6(9), 8165-8189. https://doi.org/10.3390/rs6098165
28. Huld, T. (2017). PVMAPS: Software tools and data for the estimation of solar radiation and photovoltaic module performance over large geographical areas. Solar Energy, 142, 171-181. https://doi.org/10.1016/j.solener.2016.12.014
29. https://globalsolaratlas.info
30. Nebey, A. H., Taye, B. Z., & Workineh, T. G. (2020). Site Suitability Analysis of Solar PV Power Generation in South Gondar, Amhara Region. Journal of Energy, 3519257. https://doi.org/10.1155/2020/3519257
31. Al Garni, H. Z., & Awasthi, A. (2017). Solar PV power plant site selection using a GIS-AHP based approach with application in Saudi Arabia. Applied Energy, 206, 1225-1240. https://doi.org/10.1016/j.apenergy.2017.10.024
32. Li, D. (2013). Using GIS and Remote Sensing Techniques for Solar Panel Installation Site Selection. [Master's thesis, University of Waterloo]. https://doi.org/10.1016/j.solener.2006.07.009
33. Tahri, M., Hakdaoui, M., & Maanan, M. (2015). The evaluation of solar farm locations applying Geographic Information System and Multi-Criteria Decision-Making methods: Case study in southern Morocco. Renewable and sustainable energy reviews, 51, 1354-1362. https://doi.org/10.1016/j.rser.2015.07.054
34. Al-Shammari, S., Ko, W., Al Ammar, E. A., Alotaibi, M. A., & Choi, H. J. (2021). Optimal decision-making in photovoltaic system selection in Saudi Arabia. Energies, 14(2), 357. https://doi.org/10.3390/en14020357
35. Masoom, A., Kosmopolous, P., & Bansal, A. (2021). Solar Irradiance Assessment and Forecasting in Tropical Climates using Satellite Remote Sensing

and Physical Modelling (No. EMS2021-352). Copernicus Meetings. https://doi.org/10.5194/ems2021-352
36. https://www.earthdata.nasa.gov
37. https://livingatlas.arcgis.com/landcover
38. https://www.openstreetmap.org
39. Robinson, V. B. (2003). A perspective on the fundamentals of fuzzy sets and their use in geographic information systems. Transactions in GIS, 7(1), 3-30. https://doi.org/10.1111/1467-9671.00127
40. Corrente, S., Greco, S., & Słowiński, R. (2017). Handling imprecise evaluations in multiple criteria decision aiding and robust ordinal regression by n-point intervals. Fuzzy Optimization and Decision Making, 16, 127-157. https://doi.org/10.1007/s10700-016-9244-x
41. Saaty, T. L. (1977). A scaling method for priorities in hierarchical structures. Journal of mathematical psychology, 15(3), 234-281. https://doi.org/10.1016/0022-2496(77)90033-5
42. Ishizaka, A., & Labib, A. (2011). Review of the main developments in the analytic hierarchy process. Expert Systems with Applications, 38(11), 14336-14345. https://doi.org/10.1016/j.eswa.2011.04.143
43. Alhammad, A., Sun, Q., & Tao, Y. (2022). Optimal solar plant site identification using GIS and remote sensing: framework and case study. Energies, 15(1), 312.
44. https://pro.arcgis.com/en/pro-app/latest/arcpy/spatial-analyst/what-is-the-spatial-analyst-module.htm
45. Adjiski, V., Kaplan, G., & Mijalkovski, S. (2022). Assessment of the solar energy potential of rooftops using LiDAR datasets and GIS based approach. International Journal of Engineering and Geosciences, 8(2), 188-199. https://doi.org/10.26833/ijeg.1112274
46. Senkal, E., Kaplan, G., & Avdan, U. (2021). Accuracy assessment of digital surface models from unmanned aerial vehicles' imagery on archaeological sites. International Journal of Engineering and Geosciences, 6(2), 81-89. https://doi.org/10.26833/ijeg.696001